XVI International Conference on Durability of Building Materials and Components
DBMC 2023, China
K.F. Li and D.P. Fang (Eds)

Numerical Simulation on the Influences of Wind Pressure on Jet Characteristics of Shotcrete

Shuang ZHANG [1], Yanrong ZHANG [1], Kai WU [1], Xiangming KONG [2]

[1]School of Civil Engineering, Beijing Jiaotong University, Beijing 100044, China,
21121218@bjtu.edu.cn (Shuang Zhang), yr.zhang@bjtu.edu.cn (Yanrong ZHANG),
20115060@bjtu.edu.cn (Kai WU)
[2]Department of Civil Engineering, Tsinghua University, Beijing 100084, China,
kxm@mail.tsinghua.edu.cn

Abstract. *A gas-liquid two phases model of shotcrete was developed to simulate the whole process from the spouting of concrete from nozzle, the scattering in the flow field to its colliding with a wall based on computational fluid dynamics theory, in which concrete was regarded as a Bingham fluid. The influences of wind pressures、pumping speeds、air incident angles and rheological parameters on five characteristic parameters including spouting velocity, jet velocity, jet trajectory, collision velocity and distribution of shotcrete on the wall were analyzed in depth. Results showed that concrete was gradually mixed well with air in the nozzle with an increasing average velocity, and the increase of velocity was most pronounced in the contraction section of nozzle. With the increases of wind pressures and pumping speeds, the spouting velocity and spouting mass of concrete both increased. Higher wind pressure and pumping speed led to larger jet velocity and more concentrated distribution, resulting in significantly longer jet distance, higher collision velocity and larger distribution area. The collision velocity and volume fraction of concrete on the wall were distributed symmetrically along Y axis, shifting towards the direction of gravity. With the increases of air incident angles, the spouting velocity and spouting mass of concrete both decreased, the shifting to gravity is weakened and the volume fraction decreased first and then increased. When plastic viscosity decreased, the spouting velocity and spouting mass of concrete both increased, accompanying with a higher jet velocity, a longer spraying distance and a larger distribution area.*

Keywords: *Computational fluid dynamics theory; Construction parameters; Rheological parameters；Bingham fluid; Numerical simulation*

1 Introduction

Shotcrete possesses characteristics such as rapid strength growth, strong bonding force, high density, and high impermeability, making it an essential component of tunnel support structures. However, limitations in spray equipment, construction techniques and material properties result in significant rebounding, which not only reduces project quality but also adversely affects construction efficiency and project profits [1-4].

It has been pointed out in previous studies that the rebounding of shotcrete is closely related to the jet characteristics such as jet velocity, trajectory, and collision velocity [5-8]. In order to effectively reduce the rebound rate of concrete, researchers have conducted a series of numerical simulations and experimental studies focusing on the jet characteristics of concrete. A series of numerical simulations and experimental studies have been carried out to analyze the influence of the mix ratio of concrete, nozzle structure and construction parameters on the jet characteristics [9-14]. Pan et al. [9] conducted experiments and found that the addition of accelerator and tackifier could slightly reduce the collision velocity of shotcrete, thereby reducing the rebound rate. Su [10] and Liu [11] regarded concrete as a Newtonian fluid and found the longer the mixing section of the nozzle, the lower spouting velocity of concrete. What's more, the spouting velocity first increased and then decreased with the increase of convergence angle and length-diameter ratio of nozzle. Ginouse [12] experimentally studied the jet trajectories of concrete under different nozzle structures and found that the jet trajectories of tapering nozzle were more concentrated. Li [13] regarded concrete as a Newtonian fluid, simulated and found that with the increase of jet pressures, the concrete jet velocity increased, while the jet trajectory remained basically unchanged. Zheng [14] regarded concrete as a granular flow and studied the impact of different jet distances on the collision velocity of shotcrete, finding that the collision velocity was moderate and the rebound rate was low when the jet distance was between 0.8-1.1 m.

So far, existing simulation models usually simplify shotcrete to a Newtonian fluid or granular flow, simulating its jet velocity and trajectories at a particular stage. This simplification will inevitably lead to large deviations between the simulation results and the real situations. A gas-liquid two phases model of shotcrete was developed to simulate the whole process from the spouting of concrete from nozzle, the scattering in the flow field to its colliding with a wall based on computational fluid dynamics theory, in which concrete was regarded as a Bingham fluid. The influences of wind pressures on five characteristic parameters including spouting velocity v_1, jet velocity v_2, jet trajectory D_c, collision velocity v_3 and distribution of shotcrete on the wall V_f were used to characterize jet characteristics of shotcrete; The mechanism of different jet parameters on jet characteristics of shotcrete were investigated and compared with the results of Newtonian fluid simulation.

2 A gas-liquid two phases model of shotcrete

2.1 Eulerian model

In the Eulerian model, different phases are regarded as continuous medium with different characteristics of interpenetration and coupling, which is widely used in numerical simulations of multiphase flow fields [5, 11, 13]. The spraying process can be regarded as a continuous flow of gas-liquid two phases. Both gas and liquid phases are assumed to be continuous media, filling the entire flow field, with their flow parameters being discontinuous at the phase interface. The mass and momentum transfer at the phase interface, following the volume fraction equation, conservation of mass, conservation of momentum, and conservation of energy [13, 15].

(1) Volume fraction equation

It is assumed that *p* phase is air phase and *q* phase is concrete phase. The volume of phase *q* V_q is defined by:

$$V_q = \int_V a_q dV \tag{1}$$

Where a_q is the volume fraction of phase *q*, $\sum_{q=1}^{n} a_q = 1$; *V* is the volume of phase *q*.

The effective density of phase *q* is:

$$\hat{\rho}_q = a_q \rho_q \tag{2}$$

Where ρ_q is the physical density of phase *q*.

(2) Conservation of mass

The continuity equation for phase *q* is

$$\frac{\partial}{\partial t}(a_q \rho_q) + \nabla \cdot (a_q \rho_q \vec{v}_q) = \sum_{p=1}^{n} (\dot{m}_{pq} - \dot{m}_{qp}) + S_q \tag{3}$$

Where $\vec{v}_q$ is the velocity of phase; $\dot{m}_{pq}$ characterizes the mass transfer from the p^{th} to q^{th} phase; $\dot{m}_{qp}$ characterizes the mass transfer from phase *q* to phase *p*.

(3) Conservation of momentum

The momentum balance for phase *q* yields

$$\begin{aligned}\frac{\partial}{\partial t}(a_q \rho_q \vec{v}_q) + \nabla \cdot (a_q \rho_q \vec{v}_q \vec{v}_q) = -a_q \nabla \cdot p + \nabla \cdot \bar{\bar{\tau}}_q + a_q \rho_q \vec{g} + \\ \sum_{p=1}^{n} (\vec{R}_{pq} + \dot{m}_{pq} \vec{v}_{pq} - \dot{m}_{qp} \vec{v}_{qp}) + \\ \vec{F}_q + \vec{F}_{lift,q} + \vec{F}_{wl,q} + \vec{F}_{vm,q} + \vec{F}_{td,q}\end{aligned} \tag{4}$$

Where *p* is the pressure shared by all phases; $\bar{\bar{\tau}}_q$ is the q^{th} phase stress-strain tensor; $\vec{R}_{pq}$ is an interaction force between phases; $\vec{v}_{pq}$ and $\vec{v}_{qp}$ are the interphase velocity; $\vec{F}_q$ is an external body force; $\vec{F}_{lift,q}$ is a lift force; $\vec{F}_{wl,q}$ is a wall lubrication force; $\vec{F}_{td,q}$ is a turbulent dispersion force。

(4) Conservation of energy

To describe the conservation of energy in Eulerian multiphase applications, a separate enthalpy equation can be written for each phase:

$$\begin{aligned}\frac{\partial}{\partial t}(a_q \rho_q h_q) + \nabla(a_q \rho_q \vec{v}_q h_q) = a_q \frac{dp_q}{dt} + \bar{\bar{\tau}}_q : \nabla \vec{v}_q - \nabla \cdot \vec{q}_q + S_q + \\ \sum_{n}^{p=1} (Q_{pq} + \dot{m}_{pq} h_{pq} - \dot{m}_{qp} h_{qp}) - \nabla \cdot \sum_j h_{j,q} \vec{J}_{jq}\end{aligned} \tag{5}$$

Where h_q is the specific enthalpy of the qth; $\vec{q}_q$ is the heat flux; Q_{pq} is the intensity of heat exchange between the p^{th} and qth phase; h_{pq} and h_{qp} are the interphase enthalpy; $h_{j,q}$ is enthalpy of species *j* in phase *q*; $\vec{J}_{jq}$ is diffusive flux of species *j* in phase *q*.

2.2 Model establishment and grid generation

A Gas-liquid two phases model of shotcrete based on Eulerian model was shown in Figure 1 (a), which was composed of nozzle, flow field and wall, where the nozzle was divided into a mixing section, a contraction section and an assembling section (Figure 1 (b)). A geometric model was first created using SolidWorks software with dimensions as shown in Table 1. Then, the hexahedral mesh was generated for the geometry model using ICEM CFD, as shown in Figure 1 (c). To improve the accuracy of the model, the grid size of the nozzle was set to 0.008 m, which was set to 0.02 m in the flow field, resulting in a total of 667265 grids.

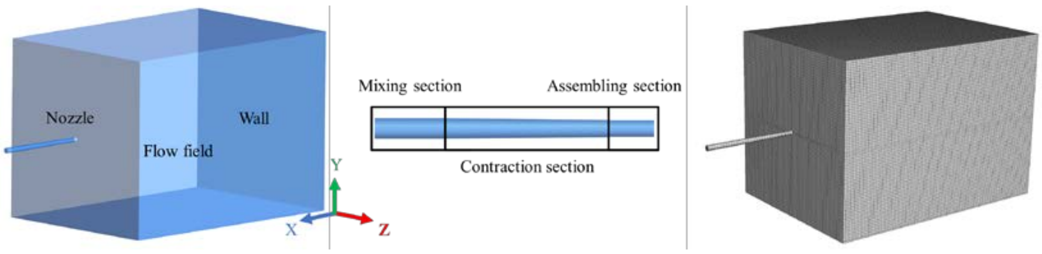

Figure 1. Gas-liquid two phases model of shotcrete

Table 1. Geometrical parameters of the nozzle, flow field and wall (size: m)

Nozzle					Flow field	Wall	
Mixing section	Contraction section	Assembling section	Diameter of inlet	Diameter of outlet	Jet distance	Width	Height
0.1	0.27	0.06	0.025	0.02	0.12	0.8	0.8

The gas phase was air at standard temperature and pressure and the liquid phase was concrete. The type of inlet boundary was set to PRESSURE_INLET and the pressure range was 0.1-1.2 MPa, which was the range commonly used in construction [16, 17]. The type of the outlet boundary was set to PRESSURE_OUTLET with the pressure of 0. The no-slip wall boundary condition is used for the wall boundary condition. The RNG model was selected to calculate the turbulent viscosity coefficient of the fluid in the flow field. The initial values of turbulence kinetic energy k and dissipation rate ε were calculated based on a turbulence intensity of 4.4% and a hydraulic diameter of 0.025 m [15]. The transient pressure-velocity coupling was adopted to solve the coupled equations of momentum and continuity. The discrete format of the momentum equation, volume fraction equation, turbulent kinetic energy equation, and turbulent dissipation coefficient equation were all solved using the first-order upwind method. The material parameters were based on the Bingham rheological parameters of the sprayed concrete in reference [18], with a plastic viscosity of 210 Pa·s, a yield stress of 190 Pa, and a density of 2380 kg·m^{-3}.

The spraying process of concrete was divided into three stages: mixing with air and spraying in the nozzle, scattering in the flow field, and colliding with the wall. In this paper, the effect of different wind pressures on the jet characteristics of shotcrete were explored by analyzing the flow velocity and trajectories of concrete.

5 characteristic parameters were extracted as shown in Figure 2. (1) Spouting velocity v_1,: velocity of concrete in the nozzle. (2) Jet velocity v_2: velocity of concrete at each point in the

flow field cross-section at Z=0. (3) Jet trajectory D_c: trajectory of concrete at each point in the flow field cross-section at Z=0. (4) Collision velocity v_3: velocity of concrete on the wall. (5) Distribution of shotcrete on the wall V_f: volume fraction of concrete on the wall.

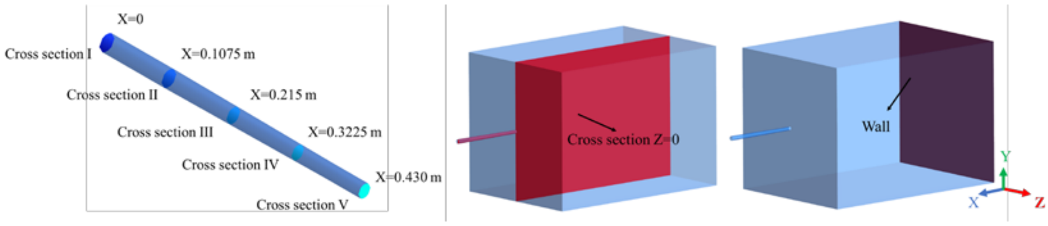

（a）Selected cross section （b）Cross section Z=0 （c）Wall

Figure 2. Schematic illustrations of extracting characteristic parameters

3 Results and discussion

3.1 Spouting velocity

The influences of wind pressures on the spouting velocity of concrete are shown in Figure 3. The velocity of concrete continuously increases from the inlet to outlet of nozzle, reaching maximum at the outlet. The velocity increases slowly in the mixing section and the assembling section, only reaching 6.03% and 3.12% respectively, while increases rapidly with a growth rate of 48.45% in contraction section. The velocity increases rapidly from 2.85 m/s to 21.67 m/s in nozzle as the wind pressure increases from 0.1 MPa to 1.2 MPa. When regard concrete as a Newtonian fluid, the spouting velocity is only 2.77 m/s under a wind pressure of 1.2 MPa.

It is well known that concrete and air gradually mixed evenly in the nozzle [10, 11, 19]. The higher the degree of homogenization from the inlet to the outlet, the faster the speed at which the concrete is propelled by the airflow. As the wind pressure increases, the pressure difference of nozzle increases, which increases the initial velocity and acceleration of the concrete, resulting a higher spouting velocity. In addition, A tapered shape of contraction section promote the mixing of air and concrete, which facilitates the air to carry the concrete to be sprayed, resulting significant increase in velocity. When regard concrete as a Newtonian fluid, it tends to collapse and flow as a whole under the influence of gravity with 0 yield stress, making it difficult to mix with air sufficiently and achieve higher spouting velocity.

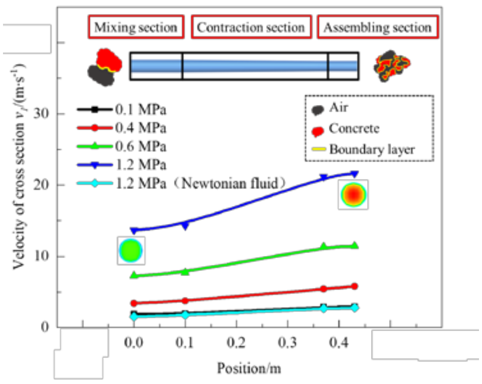

Figure 3. Average velocity of shotcrete in nozzle under different wind pressures

3.2 Jet velocity

The influences of wind pressures on the jet velocity of concrete are shown in Figure 4. When the wind pressure increases, the jet velocity of concrete increases and the distribution becomes more concentrated. When the wind pressure is 0.1 MPa, the maximum jet velocity of concrete is only 4.99 m/s , which is 33.81 m/s as which increases to 1.2 MPa. When concrete is considered as a Newtonian fluid, the maximum jet velocity is only 3.68 m/s at 1.2 MPa wind pressure.

It can be observed that the higher wind pressure, the higher spouting velocity, resulting a higher jet velocity combined with Figure 3. What's more, with the improvement of jet velocity under high wind pressures, the time of the vertical acceleration caused by gravity is shorter. Consequently, concrete sprays at the wall with a concentrated jet. The conclusion is consistent with the results reported in reference [13]. The jet velocity decreases caused by low spouting velocity when regard concrete as a Newtonian fluid.

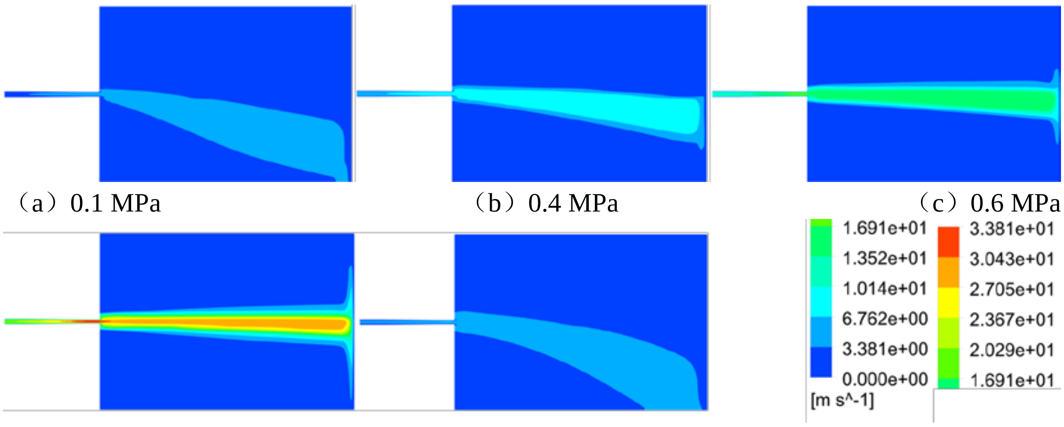

（a）0.1 MPa （b）0.4 MPa （c）0.6 MPa

（d）1.2 MPa （e）1.2 MPa（Newtonian fluid）

Figure 4. Jet velocity of shotcrete under different wind pressures

3.3 Jet trajectory

The influences of wind pressures on the jet trajectories of concrete are shown in Figure 5. There are short jet distances and limited spray qualities when the wind pressures are low. While air carries a large amount of concrete, spraying it in the form of a long and narrow beam as the wind pressures are high.

The jet trajectories in the fluid field are determined by spray qualities and jet velocity. The spray qualities can be calculated based on the product of the volume fraction of concrete and its density within all the cells at the outlet of nozzle as shown in Table 2 for different wind pressures. Combined with figure 4, the spray qualities and jet velocity are both low and the influences of gravity have a significant impact, resulting short-range concrete jets. As the wind pressure increases, the spray qualities and jet velocity gradually increase, and the influences of gravity weaken. Finally, concrete is sprayed in the form of narrow beam with high spray qualities. When considering concrete as a Newtonian fluid, the uniformity of the mixture between the concrete and air is low. The lower jet velocity and smaller qualities of concrete result in a significantly shortened jet trajectories.

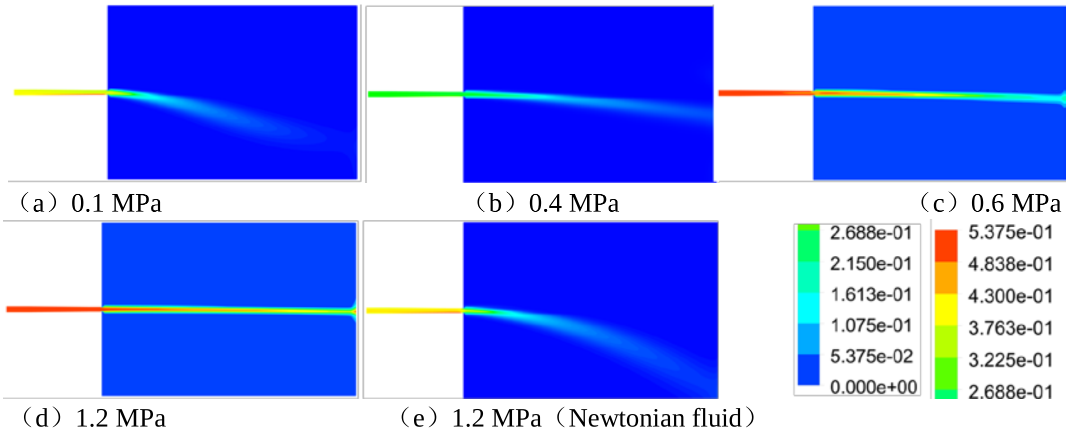

Figure 5. Jet trajectories of shotcrete under different wind pressures

Table 2. Mass of shotcrete at nozzle outlet

Wind pressure / MPa	0.1	0.4	0.6	1.2	1.2（Newtonian fluid）
Mass / kg	0.1171	0.1179	0.1185	0.1202	0.1163

3.4 Collision velocity

The influences of wind pressures on the collision velocity of concrete are shown in Figure 6. The collision velocity is symmetric along Y-axis and shifts towards the direction of gravity. The higher the wind pressure, the greater the collision velocity. When the wind pressure is 1.2 MPa, the maximum collision velocity reaches 15.1 m/s, which is much higher than 2.6 m/s at 0.1 MPa. As the wind pressure increases, the distribution area of collision velocity significantly expands and the shifting decreases. When concrete is considered as a Newtonian fluid, the maximum impact velocity of the concrete is as low as 2.2 m/s with a significant downward shifting.

The variation of collision velocity with wind pressures corresponds to the variation of jet velocity and trajectories. Higher jet velocity and concentrated jet trajectories lead higher collision velocity and lower shifting, and the expansion of the collision velocity distribution areas are mainly due to the increase of the jet flow of concrete under the high wind pressures. When considering concrete as a Newtonian fluid, the lower jet velocity and short-range injection result in a significant decrease in the collision velocity of concrete and an obvious deviation.

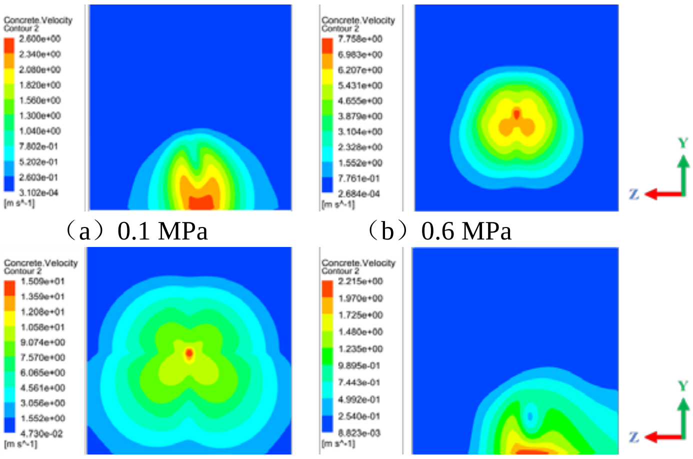

（a）0.1 MPa （b）0.6 MPa

（c）1.2 MPa （d）1.2 MPa（Newtonian fluid）

Figure 6. Collision velocity of shotcrete under different wind pressures

3.5 Distribution of shotcrete on the wall

The influences of wind pressures on distribution of shotcrete on the wall are shown in Figure 7. The distribution of shotcrete on the wall is symmetric along Y-axis and shifts towards the direction of gravity. The distribution area of concrete on the wall gradually increases, and the collision center moves upward along Y-axis with the increase of wind pressure. The distribution area is almost 0 when the wind pressure is 0.1MPa, which is 0.13 m^2 at 1.2 MPa. When concrete is assumed to be a Newtonian fluid, the distribution area of shotcrete is almost 0.

The influences of wind pressure on volume fraction i.e. the jet thickness, is shown in Figure 8. The volume fraction of concrete on the wall is symmetric along Y-axis and shifts towards the direction of gravity. As the wind pressure increases, the volume fraction of concrete and the thickness on the wall increase, while the peak shifting decreases. When the wind pressure is 0.1 MPa, the concrete volume fraction peaks at 0.26 m and the shifting along Y-axis is 3.01%. While the peak value reaches 0.015 m and the shifting is 51.7% at 1.2 MPa.

The increase in both distribution range and volume fraction of concrete is attributed to the increase in spray qualities and collision velocity under high wind pressure; The shifting of collision center and peak is mainly caused by changes in the trajectories of concrete spraying under different wind pressures.

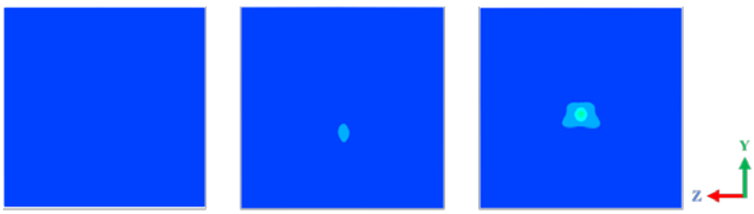

（a）0.1 MPa （b）0.4 MPa （c）0.6 MPa

（d）1.2 MPa （e）1.2 MPa（Newtonian fluid）

Figure 7. Distribution of shotcrete on the wall under different wind pressures

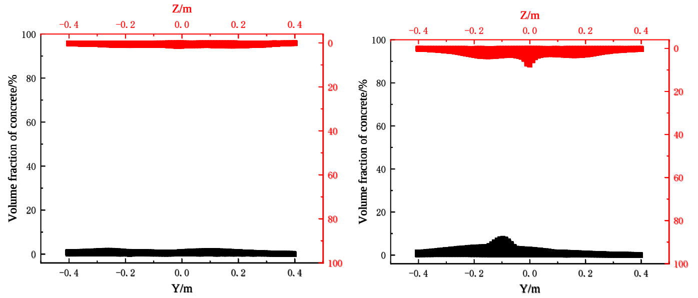

（a）0.1 MPa （b）0.4 MPa

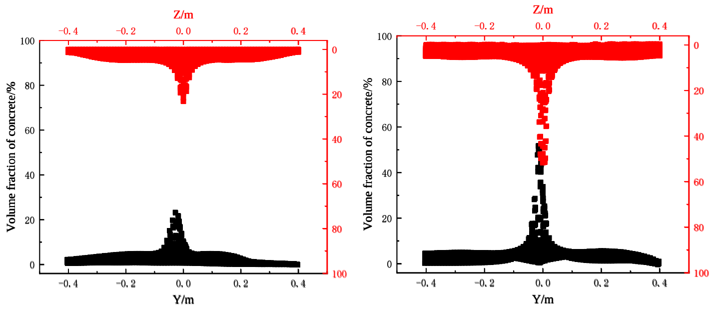

（c）0.6 MPa （d）1.2 MPa

Figure 8. Volume fraction of shotcrete on the wall under different wind pressures

4 Conclusions

1) The concrete and air are gradually mixed uniformly and the average velocity increases from the inlet to the outlet of nozzle, with the most significant increase in the contraction section. The air pressure increases from 0.1 MPa to 1.2 MPa, and the spouting velocity of concrete increases from 2.85 m/s to 21.67 m/s with the spraying qualities increases.

2) At low wind pressures, the lower spouting velocity and spraying qualities result in a significant decrease in jet velocity and jet distance of concrete in the flow field. As the wind pressure increases, the spraying qualities and jet velocity of concrete gradually increase, and the influence of gravity weakens. Eventually, concrete is sprayed in a long and narrow beam.

3) The collision velocity and volume fraction of concrete on the wall are symmetrically distributed along the Y-axis and shift towards the direction of gravity. As the wind pressure increases, the collision velocity increases, the shifting decreases, and the distribution area increases. Moreover, the volume fraction of concrete on the wall increases significantly (the peak value increases from 3.01% to 51.7%). This is mainly due to changes of spraying qualities, jet velocity and trajectories under different wind pressures.

4) The five jet characteristic parameters obtained from the simulation of concrete as a Bingham fluid are much higher than that of a Newtonian fluid. We are currently conducting

research on the effects of regarding concrete as a discrete medium and investigating the influence of nozzle parameters on the characteristics of sprayed concrete jetting.

References

QIAO Liwei. *Optimization of Structural Setting Based on Forced Ventilation Method in Tunnel Under Construction*. Journal of Southwest Jiaotong University, 2018, 53(06): 1245-1252, 1277.

ZHAO Wenbin, TAN Yunzhen, SHANG Yandong, et al. *The mechanism analysis of shotcrete concrete additive used in coal mines*.Journal of China Coal Society, 2009, 34(04): 526-530.

ZENG Xiantao, REN Zhenhua，Wang Xingguo. *Experimental investigations on reducing the dust density and the rebound rate of shotcrete by using magnetized water*. Journal of China Coal Society, 2014, 39(04): 705-712.

CHEN Lianjun, LIU Xianguo. *Evaluation indexes and flow field simulation of mine concrete wet spraying nozzle*. Coal Engineering, 2017, 49(04): 101-104.

LI Pengcheng. *Study on experiment and numerical simulation of collision-rebound of wet-mix shotcrete*.Qingdao: Shandong University of Science and Technology. College of Energy and Mining Engineering, 2019: 1-28.

NING Fengwei, DING Jiantong, BAI Yin, et al. *Advance of study on factors of influences on rebound rate of wet shotcrete*. Water Resources and Hydropower Engineering, 2018, 49(1): 149-155.

Chen Lianjun, Sun Zhenjao, Liu Guoming, et al. *Spraying characteristics of mining wet shotcrete*. Construction and Building Materials, 2022, 316: 125888.

SU Chang, WU Zhuang, ZHENG Xiaokui. *Analysis of Rebound Rate of Wet Shotcrete Based on Experiment and Discrete Element Method*. Shock and Vibration, 2022, 2022.

PAN Gang, LI Pengcheng, CHEN Lianjun, et al. *A study of the effect of rheological properties of fresh concrete on shotcrete-rebound based on different additive components*. Construction and Building Materials, 2019, 224: 1069-1080.

SU Chang, ZHENG Qiangqiang, ZHAO Wukun. *A combined experimental and numerical study of shotcrete jets and related wet spray nozzles*. Fluid Dynamics & Materials Processing, 2020, 16(05): 947-960.

LIU Cao. *Mixed fluid evenness study of flow field of wet concrete spraying machine nozzle*. Changsha: Central South University. College of Mechanical and Electrical Engineering, 2013: 42-48.

GINOUSE N, JOLIN M, BISSONNETTE B. *Effect of equipment on spray velocity distribution in shotcrete applications*[J]. Construction and Building Materials, 2014, 70: 362-369.

LI Aimin. *Research on Key Technologies of wet-mix shotcreting system for coal mine entry*. Xuzhou: China University of Mining and Technology. College of Mechanical and Electrical Engineering, 2015: 59-70.

ZHENG Xiaokui. *Research on rebound rate of wet shotcrete based on discrete element method*. Huainan: Anhui University of Science and Technology. College of Mechanical Engineering, 2021: 25-27.

WANG Fujun. *Computational fluid dynamics analysis*. Beijing: Tsinghua University Press, 2004: 31-51.

REN Wei. *Control measures for rebound rate of shotcrete in tunnel*. Transpoworld, 2021(23): 167-168.

TU Jianshan, GAO Ming. *Cause analysis and measures for high rebound rate of concrete spraying*. Safety in Coal Mines, 2004(02): 21-22.

ZHANG Ge. *Performance improving mechanism and mix design method of shotcrete*. Beijing: Beijing Jiaotong University. School of Civil Engineering, 2021: 92-94.

GINOUSE N, JOLIN M. *Investigation of spray pattern in shotcrete applications*. Construction and Building Materials, 2015, 93: 966-972.